Canonical Piecewise-Linear Representation of Curves in the Wave Digital Domain

Alberto Bernardini and Augusto Sarti

Dipartimento di Elettronica, Informazione e Bioingegneria (DEIB)

Politecnico di Milano, Piazza L. Da Vinci 32, 20133 Milano – Italy

[alberto.bernardini,augusto.sarti]@polimi.it

Abstract—**Global, explicit representations of nonlinearities are desirable when implementing nonlinear Wave Digital (WD) structures, as they free us from the burden of managing look-up tables, performing data interpolation and/or using iterative solvers. In this paper we present a method that, starting from certain parameterized PieceWise-Linear (PWL) curves in the Kirchhoff domain, allows us to express them in the WD domain using a global and explicit representation. We will show how some curves (multi-valued functions in the Kirchhoff domain) can be represented as functions in canonical PWL form in the WD domain. In particular, we will present a procedure, which, in the most general case, also returns the conditions on the reference port resistance under which it is possible to find explicit mappings in the WD domain.**

I. INTRODUCTION

Wave Digital (WD) structures are known to be very effective for building stable and efficient digital filters [1] and digitally emulating physical systems which can be represented as analog circuits [2]. For these reasons, they proved to be suitable for Virtual Analog modeling [3], [4]. WD structures are based on the linear port-wise transformation (1)

$$a = v + R\,i \qquad b = v - R\,i \quad , \tag{1}$$

which maps Kirchhoff (K) variables, i.e. port voltage v and port current i, into WD variables (scattering waves), i.e. incident wave a and reflected wave b, R being a free parameter called port resistance. Most WD structures with one nonlinear (NL) element [5], [6] can be efficiently implemented in a systematic fashion [7]. NL WD elements are generally implemented using look-up tables [8] or iterative solvers [9], even though alternative techniques exist [10]. However, disposing of canonical PieceWise Linear (PWL) representations [11] of nonlinearities in the WD domain would be very useful for many reasons. The main reason is that canonical PWL representations are global and explicit; therefore, they eliminate the need of using look-up tables and/or iterative techniques for computing the reflected waves, leading to implementations with low computational cost and low storage requirements. Moreover, they are extremely flexible, as they allow us to model the nonlinearity with arbitrary accuracy, tuning the number of vertexes and segments accordingly. Some papers in the literature present PWL representations of nonlinearities in the WD domain [8], [12], [13]; however, a global PWL representation appears only in [5]. Nevertheless, as will be

outlined in this paper, the formulas in [5] are valid only in a limited number of cases.

In Section II of this paper we will describe the canonical PWL representation of a scalar nonlinearity in the WD domain. In Section III we will provide a generalized version of the theoretical contributes offered in [8] and [5] that describe the conditions under which it is possible to derive explicit wave mappings, starting from parametrized curves in the K domain. In Section IV we will present a novel procedure that, given ordered vectors of vertex coordinates of a PWL curve in the K domain, returns the ranges of values of the port resistance allowing us to find an explicit wave mapping. Moreover, if an explicit wave mapping exists, it is shown how a canonical PWL representation can be derived. Section V shows that the procedure presented in Section IV lead to simplified conditions on the port resistance if applied to monotonic increasing and decreasing functions in the K domain. Finally, examples of applications to the Shockley diode model and the Chua's resistor are shown.

II. CANONICAL PWL REPRESENTATION

A canonical PWL representation for a generic single-valued wave mapping $b = h(a)$ with a finite number of jump discontinuities can be written as [11]

$$b = \mu_0 + \mu_1 a + \sum_{j=1}^{N} \left(\eta_j |a - a_j| + \nu_j \mathrm{sgn}\,(a - a_j) \right) \tag{2}$$

where $|.|$ indicates the absolute value, sgn is the sign function, $N+1$ is the number of segments (from the leftmost with index $j = 0$ to the rightmost with index $j = N$), N is the number of vertices with coordinates (a_j, b_j) (from the leftmost with index $j = 1$ to the rightmost with index $j = N$) and

$$
\begin{aligned}
&\mu_1 = 0.5\,(m_0 + m_N)\\
&\eta_j = 0.5\,(m_j - m_{j-1}) \quad j = 1, \dots, N\\
&\nu_j = \begin{cases} 0 \;, & \text{if } f_b(a) \text{ is continuous at } a = a_j\\ 0.5\left(h\left(a_j^+\right) - h\left(a_j^-\right)\right) \;, & \text{otherwise} \end{cases}\\
&\mu_0 = h(0) - \sum_{j=1}^{N} \left(\eta_j |a_j| - \nu_j \mathrm{sgn}\,(a_j) \right)
\end{aligned}
$$

where m_j is the slope of the j-th segment and it is defined as

$$m_j = \frac{b_{j+1} - b_j}{a_{j+1} - a_j} \;, \quad j = 1, \dots, N-1 \;. \tag{3}$$

For the sake of simplicity, but without loss of generality, let us assume the slopes of the leftmost and the rightmost segments, corresponding to the intervals $[-\infty, a_1]$ and $[a_N, +\infty]$, to be $m_0 = m_1$ and $m_N = m_{N-1}$, respectively. However, in general, it is possible to obtain a canonical PWL representation in the form (2) if and only if

$$a_1 \le a_2 \le \cdots \le a_N \qquad (4)$$

which, again, corresponds to saying that the function h must be single-valued and with a finite number of jump discontinuities. The WD domain coordinates are grouped in the two vectors $\mathbf{a_p} = [a_1, \ldots, a_N]^T$, where T denotes transposition, and $\mathbf{b_p} = [b_1, \ldots, b_N]^T$, which will be used in the following Sections.

III. FROM A CURVE IN THE KIRCHHOFF DOMAIN TO AN EXPLICIT WAVE MAPPING

A general method based on parametrization, for finding explicit wave mappings in canonical form, can be formalized combining the theoretical findings offered in [5] and [8]. Let us start from a generic PWL curve in the K domain, i.e. in the voltage-current $v - i$ plane. The curve is composed of $N+1$ segments and N vertices with coordinates (v_k, i_k) being $1 \le k \le N$. The set of coordinates $\{(v_1, i_1), \ldots, (v_N, i_N)\}$ is ordered according to an oriented path, which follows the curve characteristic. In general, this can be done by introducing a parameterization of the curve, as explained in [11] (see Section II.C, p. 919) with generic PWL unicursal curves. Parameterizing the curve means obtaining two single-valued functions in the form $v(\rho)$ and $i(\rho)$, where ρ is a common parameter. Therefore, the coordinates of each vertex are obtained as $v_k = v(\rho_k)$ and $i_k = i(\rho_k)$ with $\rho_k > \rho_{k-1}$ and $1 < k \le N$. If the reference curve is a current-controlled or a voltage-controlled single-valued function (with a finite number of jump discontinuities), ordering the set of coordinates is straightforward, as we set $\rho = i$ or $\rho = v$. Now, according to (1) we can express the wave variables as

$$\begin{aligned} a &= f_a(\rho) = v(\rho) + R\,i(\rho) \\ b &= f_b(\rho) = v(\rho) - R\,i(\rho) \end{aligned} \qquad (5)$$

where f_b and f_a are NL functions of ρ. An explicit wave mapping can be found if and only if f_a admits an inverse f_a^{-1} such that

$$b = f_b\left(f_a^{-1}(a)\right) . \qquad (6)$$

f_a is invertible, if it is strictly monotonic. However, as canonical forms can accommodate also jump discontinuities [11], traditional conditions on f_a, discussed in the literature [5], [8], can be relaxed; it suffices that f_a be either a non-decreasing or a non-increasing function. Therefore, setting $\delta v_k = (v_{k+1} - v_k)$ and $\delta i_k = (i_{k+1} - i_k)$, one of the following two conditions must be met

$$\delta v_k + R\,\delta i_k \ge 0 \qquad (7)$$

$$\delta v_k + R\,\delta i_k \le 0 \qquad (8)$$

for each $1 \le k < N$. As our goal is to derive a function h in canonical PWL form (2), such that $h(a) = f_b\left((f_a^{-1}(a))\right)$,

we need to find the coordinates (a_j, b_j), which satisfy (4). In order to do this, let us define the vectors of coordinates $\mathbf{v_p} = [v_1, \ldots, v_N]^T$ and $\mathbf{i_p} = [i_1, \ldots, i_N]^T$, such that the corresponding points in the WD domain have coordinates

$$\tilde{\mathbf{a}}_\mathbf{p} = \mathbf{v_p} + R\,\mathbf{i_p} \qquad \tilde{\mathbf{b}}_\mathbf{p} = \mathbf{v_p} - R\,\mathbf{i_p} \qquad (9)$$

where $\tilde{\mathbf{a}}_\mathbf{p} = [\tilde{a}_1, \ldots, \tilde{a}_N]^T$ and $\tilde{\mathbf{b}}_\mathbf{p} = [\tilde{b}_1, \ldots, \tilde{b}_N]^T$ are not necessarily equal to vectors $\mathbf{a_p}$ and $\mathbf{b_p}$, already defined in Section II. In particular, it can be easily verified that if condition (7) is met, the set of points in the WD domain is characterized by non-decreasing a-coordinates. Therefore, as (4) holds, we set $\mathbf{a_p} = \tilde{\mathbf{a}}_\mathbf{p}$ and $\mathbf{b_p} = \tilde{\mathbf{b}}_\mathbf{p}$. Conversely, if (8) is met, the set of points in the WD domain is characterized by non-increasing a-coordinates and in order to satisfy (4), we need to set $\mathbf{a_p} = \mathbf{Q}\,\tilde{\mathbf{a}}_\mathbf{p}$ and $\mathbf{b_p} = \mathbf{Q}\,\tilde{\mathbf{b}}_\mathbf{p}$, where $\mathbf{Q}$ is a permutation matrix with all ones in the counter-diagonal, i.e. $\mathbf{Q}$ flips the order of the elements of the multiplied vector. As far as we know, this last consideration has never been mentioned in the literature.

IV. CONDITIONS ON THE PORT RESISTANCE

In this Section we present a procedure that, given an ordered set of points on a curve in the K domain, returns the range of all port resistances for which it is possible to obtain a corresponding wave mapping in canonical PWL form. The returned range might also include negative port resistances, which are not used in traditional WD filters. The returned range might also be the empty set. The procedure is fully general and it works for whichever kind of PWL curve. In particular, in two separated Subsections, we will show how to find the values of the port resistance R satisfying (7) or (8). As a guiding example, let us consider the PWL curve on the $v-i$ plane in Fig. 1 on the left. It is a multi-valued function, both if we consider i or v as independent variables. The relative ordered vectors of coordinates are the following

$$\mathbf{v_p} = [-0.5, -0.7, -0.9, -1.5, -0.45, 0, 0.95, 1.5, 0.8, 0.7]^T$$
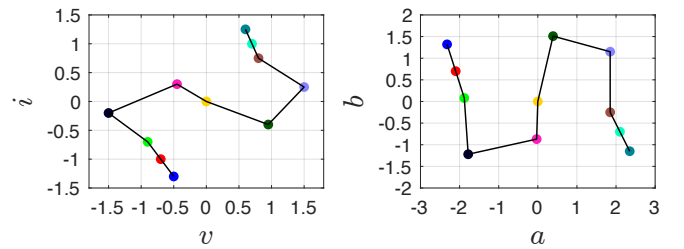$$\mathbf{i_p} = [-1.3, -1, -0.7, -0.2, 0.3, 0, -0.4, 0.25, 0.75, 1, 1.25]^T .$$

Fig. 1. On the left a PWL curve in the Kirchhoff domain. On the right the corresponding transformed curve in the WD domain representable in canonical PWL form. The chosen port resistance is $R = 1.4$.

A. Non-decreasing case

We want to find the range of values of R satisfying condition (7), that can be rewritten as

$$\begin{cases} R \ge -\delta v_k / |\delta i_k| , & \text{if } \delta i_k > 0 \\ R \le +\delta v_k / |\delta i_k| , & \text{if } \delta i_k < 0 \end{cases} \qquad (10)$$

for each $1 < k \leq N$. It may also happen that $\delta i_k = 0$; in this case, $R > -\infty$ if $\delta v_k \geq 0$ and $R = \emptyset$ if $\delta v_k < 0$, where $\emptyset$ denotes the empty set.

Let us express the system of inequalities (10) in an alternative form, defining a vector $\tilde{\mathbf{r}} = [\tilde{r}_1, \ldots, \tilde{r}_{N-1}]^T$, such that $\tilde{\mathbf{r}} = -(\tilde{\mathbf{e}} \circ \tilde{\mathbf{q}})$ where

$$\tilde{\mathbf{e}} = [\tilde{e}_1, \ldots, \tilde{e}_{N-1}]^T = [\delta v_1/|\delta i_1|, \ldots, \delta v_{N-1}/|\delta i_{N-1}|]^T \ ,$$

$$\tilde{\mathbf{q}} = [\tilde{q}_1, \ldots, \tilde{q}_{N-1}]^T = [\text{sgn}^+(\delta i_1), \ldots, \text{sgn}^+(\delta i_{N-1})]^T \ ,$$

$\circ$ indicates the Hadamard or element-wise product and $\text{sgn}^+(x)$ returns $+1$ if $x \geq 0$ or -1 if $x < 0$.

In our example we have

$\tilde{\mathbf{e}} = [-0.667, -0.667, -1.2, 2.1, 1.5, 2.375, 0.846, -1.4, -0.4, -0.4]^T$
$\tilde{\mathbf{q}} = [1, 1, 1, 1, -1, -1, 1, 1, 1, 1]^T$
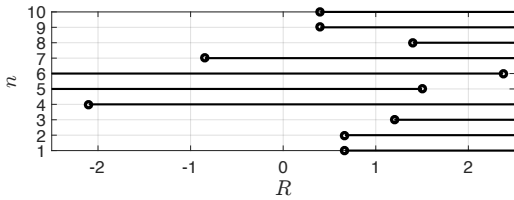$\tilde{\mathbf{r}} = [0.667, 0.667, 1.2, -2.1, 1.5, 2.375, -0.846, 1.4, 0.4, 0.4]^T \ .$

Fig. 2. Graphical representation of the system of inequalities derived from condition (7). The unknown is the port resistance R on the x-axis. The index n on the y-axis refers to the nth element of vector $\tilde{\mathbf{r}}$ and $\tilde{\mathbf{q}}$.

We now search for a range of values of R for which all the $N-1$ inequalities (7) hold. The resulting system of inequalities can be represented graphically as in Fig. 2, where circles in bold represent the elements $\tilde{r}_n$ with $1 \leq n < N$ and the black half lines indicate for each inequality the admissible range of values of R. Notice that if $\tilde{q}_n = 1$ the nth half line starts from $\tilde{r}_n$ and goes to $+\infty$; conversely, if $\tilde{q}_n = -1$ it starts from $\tilde{r}_n$ and goes to $-\infty$. Searching for a range of R values satisfying all the inequalities is now feasible, comparing all the $N-1$ ranges represented by the half lines. However, such task can be performed much more efficiently in an automatable fashion, if we reorder the elements of $\tilde{\mathbf{r}}$ and $\tilde{\mathbf{q}}$ as follows.

Let $\mathbf{r} = [r_1, \ldots, r_{N-1}]^T$ be a sorted version of $\tilde{\mathbf{r}}$, whose elements are now in non-decreasing order and let $\mathbf{P_r}$ be the corresponding permutation matrix such that $\mathbf{r} = \mathbf{P_r}\tilde{\mathbf{r}}$. We use the same permutation to reorder the elements of $\tilde{\mathbf{q}}$ and we define a vector $\mathbf{q} = [q_1, \ldots, q_{N-1}]^T$ such that $\mathbf{q} = \mathbf{P_r}\tilde{\mathbf{q}}$.

In our example we have

$\mathbf{r} = [-2.1, -0.846, 0.4, 0.4, 0.667, 0.667, 1.2, 1.4, 1.5, 2.375]^T$
$\mathbf{q} = [1, 1, 1, 1, 1, 1, 1, 1, -1, -1]^T \ .$

Fig. 3 shows the same information of Fig. 2, however it is structured according to the ordered vectors $\mathbf{r}$ and $\mathbf{q}$. In Fig. 3 the circles in bold represent the elements r_n with $1 \leq n < N$; if $q_n = 1$ the nth half line starts from r_n and goes to $+\infty$; conversely, if $q_n = -1$ it goes to $-\infty$. We notice from Fig. 3 that we can now easily find the range of R values satisfying the whole system of inequalities simply considering the half
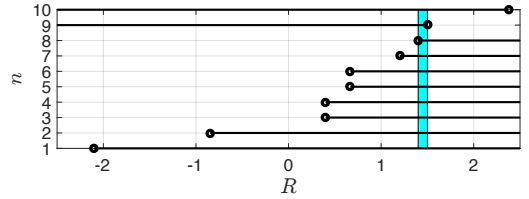

Fig. 3. Graphical representation of the system of inequalities derived from condition (7). The unknown is the port resistance R on the x-axis. The index n on the y-axis refers to the nth element of vectors $\mathbf{r}$ and $\mathbf{q}$. The colored range is the solution of the system of inequalities.

lines with indexes $n = 8$ and $n = 9$, as all the elements of $\mathbf{q}$ up to $q_8 = 1$ are equal to 1, $q_9 = q_{10} = -1$ and the elements of $\mathbf{r}$ are in a non-decreasing order by definition. Therefore, the searched range of values is $1.4 \leq R \leq 1.5$, as it can be verified by looking at Fig. 3.

Notice that, in general, a suitable range of R values exists if and only if ones and minus ones in vector $\mathbf{q}$ are in two separable subvectors made of consecutive elements of $\mathbf{q}$ and the subvector of ones precedes the subvector of minus ones. Such subvectors can also be empty. More precisely, we can find exactly the range of port resistances satisfying (8) as

$$\begin{cases} r_n \leq R \leq r_{n+1} \ , & \text{if } (q_n - q_{n+1}) = 2 \text{ and } [q_n, q_{n+1}] \text{ is} \\ & \text{the only pair of consecutive elements} \\ & \text{of } \mathbf{q} \text{ such that } |q_n - q_{n+1}| = 2 \\ R \leq r_1 \ , & \text{if } q_k = -1 \text{ for each } k \\ R \geq r_{N-1} \ , & \text{if } q_k = +1 \text{ for each } k \\ R = \emptyset \ , & \text{otherwise} \ . \end{cases}$$
(11)

where $1 \leq k < N$ and $1 \leq n < N$.

Going back to our example, let us set $R = 1.4$, so that, applying (9), we can find the following vectors of coordinates in the WD domain

$\tilde{\mathbf{a}}_\mathbf{p} = [-2.32, -2.1, -1.88, -1.78, -0.03, 0, 0.39, 1.85, 1.85, 2.1, 2.35]^T$
$\tilde{\mathbf{b}}_\mathbf{p} = [1.32, 0.7, 0.08, -1.22, -0.87, 0, 1.51, 1.15, -0.25, -0.7, -1.15]^T$

As condition (7) is met, i.e. we are in the non-decreasing case, we can set $\mathbf{a}_\mathbf{p} = \tilde{\mathbf{a}}_\mathbf{p}$ and $\mathbf{b}_\mathbf{p} = \tilde{\mathbf{b}}_\mathbf{p}$. Fig. 1 on the right shows the resulting explicit wave mapping. As we set R equal to one of the two interval limits of the allowed range $1.4 \leq R \leq 1.5$, we expect a jump discontinuity appearing in the PWL wave mapping; in fact, we have $a_8 = a_9 = 1.85$. As mentioned in Section II, jump discontinuities can be handled in a global and explicit fashion, if a canonical PWL representation of $b = h(a)$ is used (2).

B. Non-increasing case

Similarly to what done in Subsection IV-A, we want to find the range of values of R satisfying condition (8), that can be rewritten as

$$\begin{cases} R \leq -\delta v_k/|\delta i_k| \ , & \text{if } \delta i_k > 0 \\ R \geq +\delta v_k/|\delta i_k| \ , & \text{if } \delta i_k < 0 \end{cases}$$
(12)

for each $1 \leq k < N$. It may also happen that $\delta i_k = 0$; in this case, $R = \emptyset$ if $\delta v_k \geq 0$ and $R < +\infty$ if $\delta v_k < 0$.

Let us introduce the vector $\mathbf{d} = [d_1, \ldots, d_{N-1}]^T$, defined as $\mathbf{d} = -\mathbf{q}$, in addition to the already described vector $\mathbf{r}$. In our example of Fig. 1 we have

$$\mathbf{d} = [-1, -1, -1, -1, -1, -1, -1, -1, 1, 1]^T$$

The resulting system of inequalities is graphically represented in Fig. 4, where circles in bold represent the elements r_n with $1 \le n < N$ and the black half lines indicate for each inequality the admissible range of values of R. Notice that if $d_n = 1$ the nth half line starts from r_n and goes to $+\infty$; conversely, if $d_n = -1$ it starts from r_n and goes to $-\infty$.
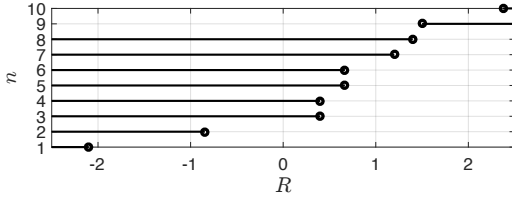

Fig. 4. Graphical representation of the system of inequalities derived from condition (8). The unknown is the port resistance R on the x-axis. The index n on the y-axis refers to the nth element of vectors $\mathbf{r}$ and $\mathbf{d}$.

Notice from Fig. 4 that no R satisfies the system of inequalities. This is apparent if we look at vector $\mathbf{d}$, which is composed of a subvector of minus ones followed by a subvector of ones.

In general, we can exactly find the range of port resistances satisfying (8) as

$$\begin{cases} r_n \le R \le r_{n+1}\,, & \text{if } (d_n - d_{n+1}) = 2 \text{ and } [d_n, d_{n+1}] \text{ is} \\ & \text{the only pair of consecutive elements} \\ & \text{of } \mathbf{d} \text{ such that } |d_n - d_{n+1}| = 2 \\ R \le r_1\,, & \text{if } d_k = -1 \text{ for each } k \\ R \ge r_{N-1}\,, & \text{if } d_k = +1 \text{ for each } k \\ R = \emptyset\,, & \text{otherwise}\,. \end{cases} \tag{13}$$

V. EXAMPLES OF APPLICATION

A. Monotonically increasing functions

Monotonically increasing functions in the K domain can be always parameterized by v or i (voltage-controlled case or current-controlled case). Let us assume that, once the independent variable is chosen, the coordinates of the vertexes are put in increasing order, starting from lower values. In that case, $\delta v_k > 0$ and $\delta i_k > 0$ for each $1 \le k < N$. We also assume $R > 0$, as negative port resistances are not used in traditional WD structures. It follows that, condition (7) reduces to $R \ge -\delta v_k/\delta i_k$ and it is always true. Conversely, condition (8) reduces to $R \le -\delta v_k/\delta i_k$ and it is always false for $R > 0$. Therefore, in practice, it is always possible to find an explicit wave mapping in canonical PWL form starting from monotonically increasing PWL functions in the K domain and using whichever $R > 0$. Moreover, we are always sure that condition (7) is met, while condition (8) is not; therefore, the order of the vertexes of the PWL curve is preserved passing from the K to the WD domain.
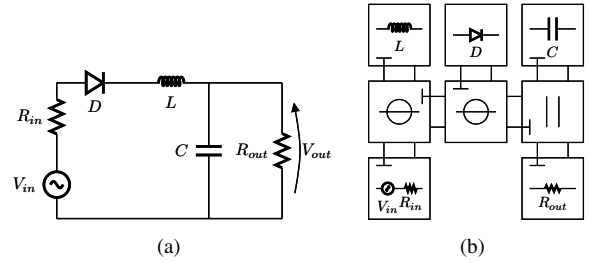

Fig. 5. Diode-based Envelope Follower. Fig. 5(a) shows the circuit in the K domain and Fig. 5(b) shows the corresponding WD structure. Parameters: $C = 10^{-7}$ F, $L = 10^{-6}$ H, $R_{out} = 5000\ \Omega$ and $R_g = 3\ \Omega$.

1) Shockley diode model: As an example, we will consider the Shockley diode model, that is characterized by the monotonically increasing function $i(v) = I_s\left(1 - e^{v/(\eta V_t)}\right)$, where I_s is the saturation current, η is the ideality factor and V_t is the thermal voltage. We will assume $I_s = 1$ pA, $\eta = 1$ and $V_t = 25$ mV. In the literature [14]–[16], a corresponding analytical wave mapping, $b = a + RI_s - 2\eta V_t\, W\left(\left(RI_s e^{(RI_s+a)/(\eta V t)}\right)/(\eta V t)\right)$, employing the Lambert function W has been proposed.
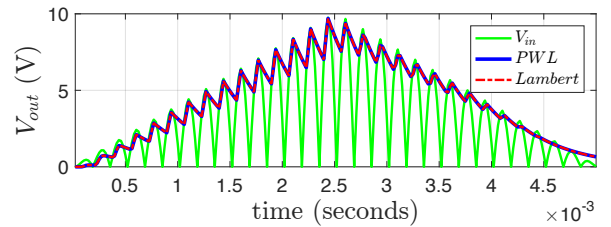

Fig. 6. Comparison between the signal V_{out} obtained with the W function approach and the same signal obtained with the PWL approach. The signal (green line) of the input generator is $V_{in} = e(t)\,|\sin(2\pi f_{in}t)|$ with $e(t) = g_{in}t/t_m$ if $t \le t_m/2$ and $e(t) = g_{in}t_m/t$ if $t > t_m/2$, where $f_{in} = 3$ kHz, $g_{in} = 20$, $t_m = 2.5$ s and sampling frequency $F_s = 48$ KHz.

Here we will compare two WD implementations in the MATLAB environment (processor 3.1 GHz Intel Core i7) of the envelope detector in Fig. 5(a). One implementation uses the wave mapping with the W function (*lambertw* in MATLAB) for implementing the diode. The other implementation is based on the canonical PWL approach (eq. (2)) and the v-coordinates of the vertices are organized in the vector $\mathbf{v_P} = [-2, -1.8, \ldots, -0.2, 0, 0.002, \ldots, 0.798, 0.8]^T$, for a total of 411 vertexes. In both cases the WD structure is the one in Fig. 5(b). As we can see from Fig. 6 the results obtained from the two implementations are very similar. However, the circuit simulation takes on average 4.75 seconds using the formula with the W function, while it takes 0.27 seconds using the proposed PWL approach.

B. Monotonically decreasing functions

Also monotonically decreasing functions in the K domain can be always parametrized by v or i. Let us assume that, the coordinates of the vertexes are put in increasing order with respect to the independent variable, starting from lower values.

Let us firstly consider the case in which i is the independent variable; we will have $\delta i_k > 0$ and $\delta v_k < 0$ for each $1 \le k < N$. Therefore, condition (7) reduces to $R \ge r_{N-1}$, where $r_{N-1} > 0$ and, being the slope of segment k defined as $\delta v_k / \delta i_k$, $-r_{N-1}$ is the slope with the largest module. Conversely, condition (8) reduces to $R \le r_1$, where $r_1 > 0$ and $-r_1$ is the slope with the smallest module.

Let us then consider the dual case in which v is the independent variable; we will have $\delta v_k > 0$ and $\delta i_k < 0$ for each $1 \le k < N$. This time, $\delta v_k / \delta i_k$ can be defined as the "reciprocal slope" of segment k. It follows that condition (7) reduces to $R \le r_1$, where $r_1 > 0$, and $-r_1$ is the "reciprocal slope" with the smallest module. Conversely, condition (8) reduces to to $R \ge r_{N-1}$, where $r_{N-1} > 0$ and $-r_{N-1}$ is the "reciprocal slope" with the largest module.

1) Chua's resistor: One common definition of the negative Chua's resistor with 4 segments is $i(v) = g_1 v + 0.5(g_0 - g_1)(|v + B_p| - |v - B_p|)$. Here we will assume $g_0 = -5 \times 10^{-4}$, $g_1 = -8 \times 10^{-4}$ and $B_p = 1$, as in [5]. We pick the v-coordinates of the vertexes as $\mathbf{v_P} = [-2, -1, 0, 1, 2]^T$. According to the previous considerations about v-controlled monotonically decreasing functions, we have that (7) is met if and only if $R \le -1/g_1$, i.e. $R \le 1250$, and (8) is met if and only if $R \ge -1/g_0$, i.e. $R \ge 2000$.

We will now implement the Chua's resistor in the WD domain, using both the explicit PWL wave mapping proposed in [5] (eq. 17) and the approach presented in this paper; then, we will compare the results. For this purpose, let us pick 48 values of R uniformly distributed in the ranges $0 < R \le 1250$ and $2000 \le R \le 3000$. Let us define the wave quantities $a = v + Ri$ and $b_{ref} = v - Ri$. Then we define b_M, which is computed using the formula in eq. 17 proposed in [5] with a as input signal, and b_B, which is computed using (2) and the approach described in this paper, again with a as input signal. Let us now sample the variable v from -5 V to 5 V with a sampling step of 0.1 for a total of 100 samples. Then we use the formula of the Chua's resistor $i(v)$ for computing the corresponding samples of i. Consequently, we can compute also the samples of the wave signals a, b_{ref}, b_M and b_B for each value of R. As we can use b_{ref} as a ground truth, let us define the error indexes $\bar{E}_M = (1/J)\sum_{j=1}^{J}|b_{refj} - b_{Mj}|$ and $\bar{E}_B = (1/J)\sum_{j=1}^{J}|b_{refj} - b_{Bj}|$, where b_{refj}, b_{Bj} and b_{Mj} are the samples of the wave signals, j is the subscript indicating the jth sample and J is the number of samples for a fixed value of R. Fig. 7 shows that, while $\bar{E}_B$ is always equal
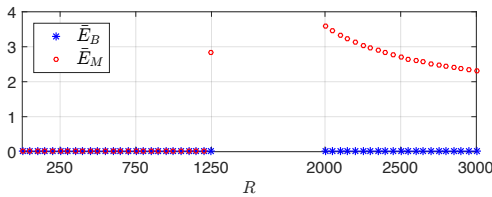

Fig. 7. Comparison of $\bar{E}_M$ and $\bar{E}_B$ for different values of R.

to 0, i.e. the proposed PWL approach always works, $\bar{E}_B$ is

much higher both for $R = 1250$ and for $R \ge 2000$. In fact, it can be verified that the formula in [5] (eq. 17) works properly only when the condition $(\delta v_k + R\,\delta i_k) > 0$ is satisfied.

VI. CONCLUSIONS AND FUTURE WORK

In this paper we presented a method for determining the values of the port resistance for which it is possible to find an explicit scalar wave mapping starting from an arbitrary PWL curve in the K domain. We also showed how to represent a curve in the WD domain using a canonical PWL representation, which is global and explicit. We are now working to extend this method to more general definitions of wave variables [17] and to multi-dimensional nonlinearities, using generalized canonical PWL representations [18].

REFERENCES

[1] A. Fettweis, "Wave digital filters: Theory and practice," *Proc. of the IEEE*, vol. 74, pp. 270–327, Feb. 1986.
[2] S. Bilbao, *Wave and Scattering Methods for Numerical Simulation*, 1st ed., J. W. . Sons, Ed., New York, July 2004.
[3] G. De Sanctis and A. Sarti, "Virtual analog modeling in the wave-digital domain," *IEEE Trans. Audio, Speech, Language Process.*, vol. 18, pp. 715–727, May 2010.
[4] M. Verasani, A. Bernardini, and A. Sarti, "Modeling Sallen-Key audio filters in the wave digital domain," in *Proc. 42nd Int. Conf. on Acoustics, Speech and Signal Process. (ICASSP)*, March 5–9 2017, pp. 431–435.
[5] K. Meerkötter and R. Scholz, "Digital simulation of nonlinear circuits by wave digital filter principles," in *IEEE Int. Symp. Circuits Syst.*, June 1989, pp. 720–723.
[6] A. Sarti and G. De Poli, "Toward nonlinear wave digital filters," *IEEE Trans. Signal Process.*, vol. 47, pp. 1654–1668, June 1999.
[7] A. Sarti and G. De Sanctis, "Systematic methods for the implementation of nonlinear wave-digital structures," *IEEE Trans. Circuits Syst. I, Reg. Papers*, vol. 56, pp. 460–472, Feb. 2009.
[8] S. Petrausch and R. Rabenstein, "Wave digital filters with multiple nonlinearities," in *Proc. European Signal Process. Conf. (EUSIPCO)*, vol. 12, Vienna, Austria, Sept. 2004.
[9] M. J. Olsen, K. J. Werner, and J. O. Smith, "Resolving grouped nonlinearities in wave digital filters using iterative techniques," in *Proc. 19th Conf. Digital Audio Effects (DAFx-16)*, Brno, Czech Republic, Sept. 5 – 9 2016.
[10] A. Bernardini and A. Sarti, "Dynamic adaptation of instantaneous nonlinear bipoles in wave digital networks," in *Proc. European Signal Process. Conf. (EUSIPCO)*, Budapest, Hungary, Aug. 29 – Sept. 2 2016.
[11] L. O. Chua and S. M. Kang, "Section-wise piecewise-linear functions: Canonical representation, properties, and applications," *Proceedings of the IEEE*, vol. 65, no. 6, pp. 915–929, June 1977.
[12] A. Bernardini, K. J. Werner, A. Sarti, and J. O. Smith, "Multi-port nonlinearities in wave digital structures," in *Proc. IEEE Int. Symp. Signals Circuits Syst. (ISSCS 2015)*, Iasi, Romania, July 9–10 2015.
[13] ——, "Modeling a class of multi-port nonlinearities in wave digital structures," in *Proc. European Signal Process. Conf. (EUSIPCO)*, Nice, France, Aug. 31 – Sept. 4 2015, pp. 669–673.
[14] R. C. D. Paiva, S. D'Angelo, J. Pakarinen, and V. Välimäki, "Emulation of operational amplifiers and diodes in audio distortion circuits," *IEEE Trans. Circuits Syst. II, Exp. Briefs*, vol. 59, pp. 688–692, Oct. 2012.
[15] K. J. Werner, V. Nangia, A. Bernardini, J. O. Smith, and A. Sarti, "An improved and generalized diode clipper model for wave digital filters," in *Proc. 139th Conv. Audio Eng. Soc. (AES)*, New York, NY, Oct. 29 – Nov. 1 2015.
[16] A. Bernardini, K. J. Werner, A. Sarti, and J. O. Smith, "Modeling nonlinear wave digital elements using the Lambert function," *IEEE Trans. Circuits Syst. I, Reg. Papers*, vol. 63, pp. 1231–1242, August 2016.
[17] A. Bernardini and A. Sarti, "Biparametric wave digital filters," *IEEE Trans. Circuits Syst. I, Reg. Papers*, vol. PP, no. 99, pp. 1–13, 2017.
[18] P. Julian, "The complete canonical piecewise-linear representation: functional form for minimal degenerate intersections," *IEEE Trans. Circuits Syst. I, Fundam. Theory Appl.*, vol. 50, no. 3, pp. 387–396, Mar. 2003.